NUMERICAL MODELING OF SPACE PLASMA FLOWS: ASTRONUM-2008
ASP Conference Series, Vol. 406, © 2009
Nikolai V. Pogorelov, Edouard Audit, Phillip Colella, and Gary P. Zank, eds.

Relativistic Simulations of Magneto-rotational Core Collapse

José A. Font,[1] Pablo Cerdá-Durán,[2] Ewald Müller,[2] and Luis Antón[1]

[1]*Departamento de Astronomía y Astrofísica, Universidad de Valencia, Dr. Moliner 50, 46100 Burjassot, Valencia, Spain*
[2]*Max-Planck-Institut für Astrophysik, Karl Schwarzschild Str. 1, 85741 Garching, Germany*

Abstract. We introduce and discuss the basic features of a new numerical code designed to handle ideal MHD flows in dynamical spacetimes in general relativity, and particularly designed to investigate the gravitational collapse of the core of massive stars leading to neutron stars or black holes. After introducing the mathematical framework for the general relativistic MHD equations and the Einstein equations (within the so-called conformal flat condition) we present results from two representative simulations of magneto-rotational stellar core collapse. Our simulations highlight the importance of genuine magnetic effects such as the magneto-rotational instability on the dynamics of the process.

1. Introduction

Understanding gravitational stellar core collapse is a long-standing problem in relativistic astrophysics (see e.g. Woosley & Janka (2005) and references therein). It is a distinctive example of a field of research where essential progress has been accomplished through numerical modelling with increasing levels of complexity in the input physics and mathematics, regarding aspects as diverse as the treatment of the hydrodynamics, gravity, magnetic fields, nuclear matter equations of state, transport, etc. Numerical studies based upon Newtonian physics are vastly developed nowadays and state-of-the-art simulations are beginning to generate successful supernova explosions. On the other hand, relativistic approaches have become routine in recent years aided by the development of conservative formulations of the general relativistic hydrodynamics equations and numerically-stable formulations of the Einstein equations (see e.g. Font (2008) and references therein). While such advances also hold true in the case of the general relativistic MHD equations (GRMHD hereafter), the development is still awaiting for a thorough numerical exploration.

In fact, it is only very recently that the first GRMHD codes able to follow the evolution of matter flows in dynamical spacetimes have been developed (Duez et al. 2005; Shibata & Sekiguchi 2005; Giacomazzo & Rezzolla 2007; Anderson et al. 2008). Here, we display our contribution to this field by discussing a new axisymmetric numerical code, comprehensively presented in Cerdá-Durán et al. (2008), able to handle ideal MHD flows in dynamical spacetimes in general relativity, and particularly designed to investigate gravitational core collapse. This code is based on the hydrodynamics code described in Dimmelmeier et al.

(2002a,b), and on its extensions discussed in Cerdá-Durán et al. (2005), Cerdá-Durán & Font (2007), and Cerdá-Durán et al. (2007), to which the readers are addressed. The Maxwell equations were already incorporated in the codes of Cerdá-Durán & Font (2007) and Cerdá-Durán et al. (2007), but only in the passive magnetic field approximation, where the contribution of the magnetic field to the energy-momentum tensor is neglected yielding no impact on the dynamics. In the new code this assumption has been relaxed and we incorporate magnetic field effects on the spacetime dynamics and the self-gravity of the fluid following the approach laid out in Antón et al. (2006).

In the remainder of the paper we present a brief summary of the mathematical framework on which the code is based along with some of its essential numerical aspects. Representative results for two magneto-rotational core collapse simulations are also reported in the final section of the article. We stress, however, that the interested reader is addressed to Cerdá-Durán et al. (2008) for a much more ample discussion of all the topics considered here. In the few equations that follow in Section 2 we use units where $c = G = 1$, Greek indices run from 0 to 3, Latin indices from 1 to 3, and we adopt the standard Einstein summation convention.

2. Framework

The evolution of a magnetized fluid is determined by the conservation law of the energy-momentum, $\nabla_\mu T^{\mu\nu} = 0$, and by the continuity equation, $\nabla_\mu J^\mu = 0$, for the rest-mass current $J^\mu = \rho u^\mu$, where ρ is the rest-mass density and u^μ the 4-velocity. As usual, symbol ∇_μ is used to indicate the covariant derivative operator. The energy-momentum tensor $T^{\mu\nu}$ of a magnetized perfect fluid can be written as the sum of the fluid part and the electromagnetic field part. In the so-called ideal MHD limit (where the fluid is a perfect conductor of infinite conductivity), the latter can be expressed solely in terms of the magnetic field b^μ measured by a comoving observer. Under this assumption and following Antón et al. (2006), we choose a set of conserved quantities given by

$$D = \rho W, \tag{1}$$

$$S_i = (\rho h + b^2) W^2 v_i - \alpha b_i b^0, \tag{2}$$

$$\tau = (\rho h + b^2) W^2 - \left(P + \frac{b^2}{2} \right) - \alpha^2 (b^0)^2 - D, \tag{3}$$

where α is the lapse function of the spacetime metric, W is the Lorentz factor, h the specific enthalpy, v_i the 3-velocity, and P the thermal pressure. With the above choice the system of conservation equations for the fluid and the induction equation for the magnetic field can be cast as a first-order, flux-conservative, hyperbolic system,

$$\frac{1}{\sqrt{-g}} \left[\frac{\partial \sqrt{\gamma} \boldsymbol{U}}{\partial t} + \frac{\partial \sqrt{-g} \boldsymbol{F}^i}{\partial x^i} \right] = \boldsymbol{S}, \tag{4}$$

for a state vector $\mathbf{U}$, flux vector $\boldsymbol{F}^i$, and source vector $\boldsymbol{S}$ whose explicit expressions can be found in Cerdá-Durán et al. (2008). Symbols g and γ indicate the

determinants of the metric and of the induced spatial 3-metric, respectively. The hyperbolic structure of Eq. (4) and the associated spectral decomposition (into eigenvalues and eigenvectors) of the flux-vector Jacobians are given in Antón et al. (2006). This information is required for numerically solving the system of equations using the class of high-resolution shock-capturing (HRSC) schemes that we have implemented in our code.

In our work Einstein's field equations are formulated and solved using the conformally flat condition (CFC hereafter), introduced by Isenberg (2008). In this approximation, the 3-metric in the ADM gauge is assumed to be conformally flat, $\gamma_{ij} = \phi^4 \hat{\gamma}_{ij}$. Under the CFC assumption the gravitational field equations can be written as a system of five nonlinear elliptic equations for the set of variables $(\phi, \alpha\phi, \beta^i)$ (see e.g. Cerdá-Durán et al. (2008) for the explicit expressions). In the previous set β^i denotes the spacetime shift vector.

As mentioned before our code solves the coupled time evolution of the equations governing the dynamics of the spacetime, the fluid, and the magnetic field in general relativity. The equations are implemented using spherical polar coordinates $\{t, r, \theta, \varphi\}$ and axisymmetry and equatorial plane symmetry is assumed. The evolution of the matter fields is handled with a HRSC scheme which updates the variables (D, S_i, τ). We have implemented various cell-reconstruction procedures which are either second-order or third-order accurate in space, namely minmod, MC, and PHM (see Toro 1999, for definitions). The time update of the state vector $\boldsymbol{U}$ relies on the method of lines in combination with a second-order accurate Runge–Kutta scheme. The numerical fluxes at cell interfaces are obtained using either the HLL single-state solver of Harten et al. (1983) or the symmetric scheme of Kurganov & Tadmor (2000). The solenoidal condition of the magnetic field is ensured with the use of the flux constraint transport method, which has been adapted to the spherical polar coordinates used in the code, and uses cell interface-centered poloidal and (because of the assumption of axisymmetry) cell-centered toroidal magnetic field components. The time discretization of the induction equation is done in the same way as for the fluid equations. Correspondingly, we use a fix-point iteration scheme in combination with a linear Poisson solver to solve the CFC nonlinear elliptic equations (for further details see Cerdá-Durán et al. (2005) and Dimmelmeier et al. (2002a)). Furthermore, the code incorporates several equations of state, ranging from simple analytical expressions to tabulated microphysical equations of state.

The interested reader is addressed to Cerdá-Durán et al. (2008) for details on the various tests passed by the code. We here simply point out that the test calculations performed demonstrate the ability of the code to properly handle all aspects appearing in the astrophysical scenarios the code is intended for, namely relativistic shocks, strongly magnetized fluids, and equilibrium configurations of magnetized neutron stars.

3. Magneto-rotational core collapse simulations

We show results from simulations of two different initial models, namely a weakly magnetized model B10 with a central magnetic field of $|B|_{\rm c} = 10^{10}\sqrt{4\pi}$ Gauss, and a strongly magnetized model B12 with $|B|_{\rm c} = 10^{12}\sqrt{4\pi}$ Gauss. In either case the progenitor is the $20M_\odot$ model of Woosley et al. (2002), to which we add a

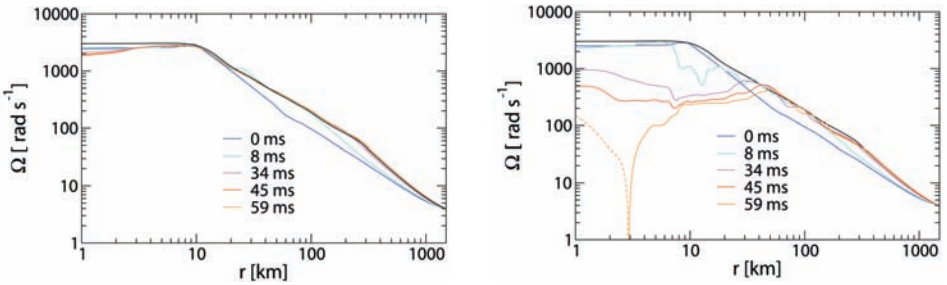

Figure 1. Radial profiles of the angular velocity Ω at the equator for model B10 (left panel) and B12 (right panel). The different lines correspond to different times after bounce: $t - t_{\rm b} = 0$, 8, 34, 45 and 59 ms. The black line displays the profile of Ω at the end of the simulation for the corresponding unmagnetized model, and is shown for comparison.

rotation profile with angular momentum $j = A^2(\Omega_c - \Omega)$ with $A = 5{\times}10^4$ km and $\Omega_c = 4.035$ s^{-1}. Therefore, both initial models are rotating almost rigidly. The magnetic field is the one generated by a circular current loop (see Jackson (1962)) at a radius of 400 km. This field has a dipolar structure far away from the center. The structure and strength of the field is fixed by two parameters, the radius of the loop and the magnetic field at the center ($r = 0$). The models are evolved with the tabulated equation of state of Shen et al. (1998) and an approximate deleptonization scheme (Liebendörfer 2005) as described in Dimmelmeier et al. (2007) and Cerdá-Durán et al. (2007). Further discussion on these results can be found in Cerdá-Durán et al. (2008).

As the collapse proceeds both the density and the magnetic energy grow very similarly for both models, because even in the highly magnetized progenitor model B12 the strength of the magnetic field is not large enough to affect the collapse dynamics. After core bounce, however, both models behave differently. On the one hand, for model B10 the magnetic field is far from saturation and grows linearly with time at the end of the simulation, while model B12 shows a saturation of the magnetic field energy shortly after core bounce. Its central density continues to grow beyond bounce, and the model eventually approaches an equilibrium configuration with a central density about 10% larger than in the weakly magnetized model.

The behavior of the central density can be understood by analyzing the profiles of the angular velocity Ω, which are plotted in Fig. 1. At the time of bounce those profiles are very similar for all models, since the magnetic field is still unimportant for the dynamics: the innermost 10 km of the core rotate rigidly, while further out Ω follows a power law with an exponent ~ -1.2. During the subsequent evolution the central region spins down, and the central density rises, the effect being more prominent in the strongest magnetized model B12 (right panel in Fig. 1). In the region $10\,{\rm km} \leq r \leq 30\,{\rm km}$ the magnetic field is strongest as differential rotation winds up the magnetic field more efficiently there (Cerdá-Durán et al. 2007). On a time scale of about 50 ms, the angular velocity decreases by about a factor 10, and the innermost few kilometers of the core even acquire retrograde rotation, an effect already observed in the Newtonian simulations of Obergaulinger et al. (2006) (see also Müller (1979)).

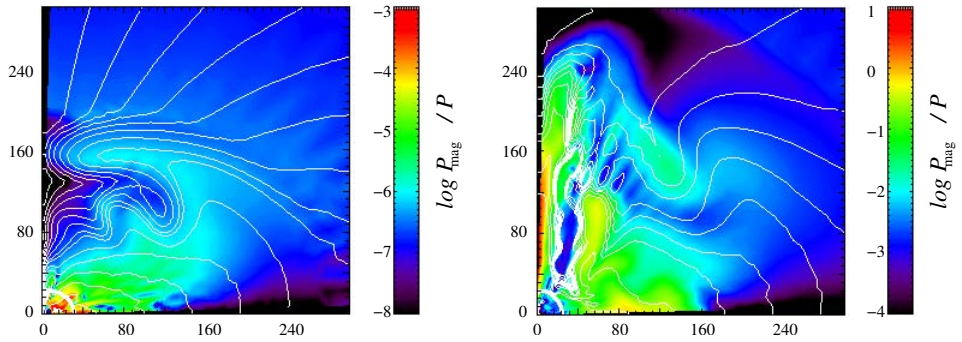

Figure 2. Structure of the magnetic field 51ms after core bounce for both models, weak field (left panel) and strong field (right panel).

The spin down of the core may be understood by means of the magneto-rotational instability (MRI hereafter; see Balbus & Hawley (1991)). In unstable regions the MRI grows exponentially for all length-scales larger than a critical length-scale $\lambda_{\rm crit} \sim 2\pi c_{\rm A}/\Omega$, where $c_{\rm A}$ is the Alfvén speed. The fastest growing MRI mode develops at length-scales near $\lambda_{\rm crit}$ on a typical time scale of $\tau_{\rm MRI} = 4\pi[\varpi\partial_\varpi\Omega]^{-1}$. Therefore, one needs to resolve length-scales of about the size of $\lambda_{\rm crit}$ in order to numerically capture the MRI. For model B12 such critical length-scale at bounce is $\lambda_{\rm crit} \sim 1\,{\rm km}\ldots 5\,{\rm km}$ inside the unstable region ($10\,{\rm km} \leq r \leq 30\,{\rm km}$). This region is covered with 60 radial and 30 angular zones, which corresponds to a resolution $(\Delta r, r\Delta\theta)$ of $125\,{\rm m}\times 500\,{\rm m}$ at $r = 10\,{\rm km}$, and $900\,{\rm m}\times 1500\,{\rm m}$ at $r = 30\,{\rm km}$. This resolution is marginally sufficient to resolve the length-scale of the fastest growing mode of the MRI at bounce ($5-10$ radial zones, and $2-3$ angular zones). The strong redistribution of the angular momentum observed for model B12 might therefore be caused by the MRI. On the other hand, for model B10 the critical length-scale at bounce is about a factor of 100 smaller, ie $\lambda_{\rm crit} \sim 10\,{\rm m}\ldots 50\,{\rm m}$, and thus the fastest growing mode of the MRI cannot be resolved with our grid resolution.

Finally, we show in Fig. 2 the magnetic field topology for both models at the end of the simulation. In the low magnetized model B10 (left panel) the (transient) prompt convection developing after bounce twists the magnetic field outside the so-called neutrino-sphere, which is assumed to be located at about 30 km. In model B12 the magnetic field grows to values near equipartition, and a distinctive, strongly magnetized outflow propagates along the axis behind the shock front. Between $10\,{\rm km} \lesssim r \lesssim 30\,{\rm km}$, where the MRI is predominantly growing, axisymmetric channel flows form, which are morphologically similar to the flows found in the accretion disk simulations of Hawley & Balbus (1992).

4. Summary

We have briefly discussed a new numerical code which solves the GRMHD equations coupled to the Einstein equations for the evolution of a dynamic spacetime. Our new numerical code is based on high-resolution shock-capturing schemes to solve the flux-conservative hyperbolic GRMHD equations, and the flux constraint transport method to ensure the solenoidal condition of the magnetic field.

The Einstein equations are formulated in the conformal flatness condition approximation, and the resulting elliptic equations are solved using a linear Poisson solver. The first application carried out with this code has been the simulation of general relativistic magneto-rotational core collapse using a realistic stellar progenitor model and a microphysical equation of state. In the near future we plan to extend the code to incorporate a simplified scheme for neutrino transport (in order to explore the post-bounce evolution of collapsing magnetized cores more reliably) along with the implementation of resistive MHD.

Acknowledgments. Research supported by the Spanish *Ministerio de Educación y Ciencia* (grant AYA2004-08067-C03-01), and by the Collaborative Research Center on *Gravitational Wave Astronomy* of the Deutsche Forschungsgesellschaft (DFG SFB/Transregio 7).

References

Anderson, M., Hirschmann, E. W., Lehner, L., et al. 2008, ArXiv e-prints, 801
Antón, L., Zanotti, O., Miralles, J. A., et al. 2006, ApJ, 637, 296
Balbus, S. A. & Hawley, J. F. 1991, ApJ, 376, 214
Cerdá-Durán, P., Faye, G., Dimmelmeier, H., et al. 2005, A&A, 439, 1033
Cerdá-Durán, P. & Font, J. A. 2007, Classical and Quantum Gravity, 24, 155
Cerdá-Durán, P., Font, J. A., & Dimmelmeier, H. 2007, A&A, 474, 169
Cerdá-Durán, P., Font, J.A., Antón, L., & Müller, E. 2008, A&A, in press
Dimmelmeier, H., Font, J. A., & Müller, E. 2002a, A&A, 388, 917
—. 2002b, A&A, 393, 523
Dimmelmeier, H., Ott, C. D., Janka, H.-T., Marek, A., & Müller, E. 2007, preprint [arXiv:astro-ph/0702305]
Duez, M. D., Liu, Y. T., Shapiro, S. L., & Stephens, B. C. 2005, Phys.Rev.D, 72, 024028
Font, J. A. 2008, Living Rev. Relativity, 11, 7
Giacomazzo, B. & Rezzolla, L. 2007, Classical and Quantum Gravity, 24, 235
Harten, A., Lax, P. D., & van Leer, B. 1983, SIAM Review, 25, 35
Hawley, J. F. & Balbus, S. A. 1992, ApJ, 400, 595
Isenberg, J. A. 2008, Int. J. Mod. Phys. D, 17, 265
Jackson, J. D. 1962, *Classical electrodynamics* (Wiley: New York)
Kurganov, A. & Tadmor, E. 2000, J. Comput. Phys., 160, 214
Liebendörfer, M. 2005, Astrophys. J., 633, 1042
Müller, E. 1979, A magnetohydrodynamic supernova model, PhD thesis, Darmstadt, Technische Hochschule
Obergaulinger, M., Aloy, M. A., Dimmelmeier, H., & Müller, E. 2006, A&A, 457, 209
Shen, H., Toki, H., Oyamatsu, K., & Sumiyoshi, K. 1998, Prog. Theor. Phys., 100, 1013
Shibata, M. & Sekiguchi, Y. 2005, Phys. Rev. D, 71, 024014
Toro, E. F. 1999, Riemann Solvers and Numerical Methods for Fluid Dynamics (Berlin: Springer Verlag)
Woosley, S. E., Heger, A., & Weaver, T. A. 2002, Rev. Mod. Phys., 74, 1015
Woosley, S. E., & Janka, H.-Th. 2005, Nature Physics, 1, 147